Cysteine-Rich Secretory Protein 3 Is a Ligand of α_1B-Glycoprotein in Human Plasma[†]

Lene Udby,*[,‡] Ole E. Sørensen,[‡] Jesper Pass,[§] Anders H. Johnsen,[||] Niels Behrendt,[§] Niels Borregaard,[‡] and Lars Kjeldsen[‡]

Granulocyte Research Laboratory, Department of Hematology, Finsen Laboratory, and Department of Clinical Biochemistry, Copenhagen University Hospital, Rigshospitalet, Copenhagen, Denmark

Received June 8, 2004; Revised Manuscript Received July 30, 2004

ABSTRACT: Human cysteine-rich secretory protein 3 (CRISP-3; also known as SGP28) belongs to a family of closely related proteins found in mammals and reptiles. Some mammalian CRISPs are known to be involved in the process of reproduction, whereas some of the CRISPs from reptiles are neurotoxin-like substances found in lizard saliva or snake venom. Human CRISP-3 is present in exocrine secretions and in secretory granules of neutrophilic granulocytes and is believed to play a role in innate immunity. On the basis of the relatively high content of CRISP-3 in human plasma and the small size of the protein (28 kDa), we hypothesized that CRISP-3 in plasma was bound to another component. This was supported by size-exclusion chromatography and immunoprecipitation of plasma proteins. The binding partner was identified by mass spectrometry as α_1B-glycoprotein (A1BG), which is a known plasma protein of unknown function and a member of the immunoglobulin superfamily. We demonstrate that CRISP-3 is a specific and high-affinity ligand of A1BG with a dissociation constant in the nanomolar range as evidenced by surface plasmon resonance. The A1BG−CRISP-3 complex is noncovalent with a 1:1 stoichiometry and is held together by strong electrostatic forces. Similar complexes have been described between toxins from snake venom and A1BG-like plasma proteins from opossum species. In these cases, complex formation inhibits the toxic effect of snake venom metalloproteinases or myotoxins and protects the animal from envenomation. We suggest that the A1BG−CRISP-3 complex displays a similar function in protecting the circulation from a potentially harmful effect of free CRISP-3.

Human cysteine-rich secretory protein 3 (CRISP-3; also known as SGP28)[1] belongs to a family of cysteine-rich secretory proteins (CRISPs) found in mammals and reptiles (*1*−*7*). The CRISPs are characterized by a high content of cysteines (16 of the 220−225 amino acids in the mature proteins are cysteine residues) and a highly conserved primary structure with 35−85% amino acid sequence identity between individual members (*2*, *7*). All of the cysteines, of which 10 are clustered in the carboxy-terminal one-fourth of the proteins, are involved in intramolecular disulfide bonds (*3*, *5*). From the structural analysis of murine CRISP-1 (*3*), the CRISPs are believed to have a two-domain structure with a large (approximately 150 residues) amino-terminal domain held together by three disulfide bridges and a smaller and compact carboxy-terminal cysteine-rich domain (approximately 50 residues) knitted together with five intradomain disulfide bonds. A domain with homology to the amino-terminal domain in CRISPs is also found in a variety of proteins from species ranging from fungi and plants to insects and mammals. The three-dimensional structure of this domain, called the SCP domain (after *s*perm *c*oating *p*rotein, which is an alternative name for murine CRISP-1), has been investigated in two species, namely, the major allergen from wasp venom (Ves v 5) and a tomato leaf protein (P14a) belonging to the pathogenesis-related proteins of group 1 (PR-1) (*8*, *9*). The SCP domain in these proteins constitutes a unique fold with an $\alpha-\beta-\alpha$ sandwich structure, which by computerized comparison was also found in the SCP domain of a human CRISP-like protein, named glioma pathogenesis-related protein (GliPR) (*10*), and thus is believed to be the general structure of SCP domains.

Despite the structural similarity between proteins with an SCP domain, a common function or mechanism of action has not been elucidated. The PR-1's are the most abundantly accumulated in plant leaves after pathogen infection or other types of stress, but despite their fungicidal activity found in vivo and in vitro, their mode of action is unknown (*11*). The proteins in insect venom are highly allergenic, but their physiological role remains elusive (*9*). Some of the CRISPs

[†] This work was supported by grants from the Danish Medical Research Council, the John and Birthe Meyer Foundation, the Novo Nordisk Foundation, and the Mauritzen la Fontaine Foundation.

* To whom correspondence should be addressed. Phone: +45 3545 4886. Fax: +45 3545 6727. E-mail: l.udby@rh.dk.

[‡] Granulocyte Research Laboratory, Department of Hematology, Copenhagen University Hospital.

[§] Finsen Laboratory, Copenhagen University Hospital.

[||] Department of Clinical Biochemistry, Copenhagen University Hospital.

[1] Abbreviations: BSA, bovine serum albumin; CRISP, cysteine-rich secretory protein; ELISA, enzyme-linked immunosorbent assay; FPLC, fast protein liquid chromatography; HSA, human serum albumin; NOG, *n*-octyl β-D-glucopyranoside; PAGE, polyacrylamide gel electrophoresis; PBS, phosphate-buffered saline; PR-1, plant pathogenesis-related protein of group 1; SCP, sperm coating protein; SDS, sodium dodecyl sulfate; SGP28, specific granule protein of 28 kDa; SVMP, snake venom metalloproteinase; TCA, trichloroacetic acid.

10.1021/bi048823e CCC: $27.50
Published on Web 09/18/2004

in lizard saliva (helothermine from *Heloderma horridum*) and snake venom (cysteine-rich venom proteins, e.g., ablomin and pseudechetoxin) are neurotoxin-like substances capable of blocking different ion-channels (*6*, *7*, *12*), but this activity is likely to reside in the carboxy-terminal cysteine-rich domain (*12*) not found in the insect and plant proteins. Of the mammalian CRISPs, CRISP-1 and CRISP-2 are primarily found in the male reproductive tract of rodents, primates, and horses. These are involved in sperm development and fusion with the oocyte (*13*, *14*). Like the reptile CRISPs, mammalian CRISP-3 (described so far only in humans, mice, and horses) is primarily a salivary gland product (*2*, *5*, *15*). Human CRISP-3 is, however, more widely distributed, and transcripts are found also in other exocrine glands (pancreas, prostate, epididymis, ovary, and colon) (*2*) and in bone marrow (*1*). We have previously isolated human CRISP-3 protein from neutrophilic granulocytes from peripheral blood and established the subcellular localization in secretory granules (specific and gelatinase granules) in these cells (*1*, *16*). By immunological methods, we have also demonstrated the presence of CRISP-3 in seminal plasma, saliva, and blood plasma (*17*). The localization of CRISP-3 in exocrine secretions covering mucous membranes and in secretory granules of phagocytes indicates a possible role of CRISP-3 in the innate immune system. This is in line with recent reports indicating that CRISP-3 is upregulated in chronic inflammation of salivary glands and pancreas and in neoplastic disease of the prostate (*18*−*20*).

By enzyme-linked immunosorbent assay (ELISA), we have previously measured the content of CRISP-3 in neutrophilic granulocytes (0.2 μg/10^6 cells) and in plasma (6.3 μg/mL) from healthy individuals (*17*). These data show that most of the CRISP-3, present in whole blood, is localized to plasma. This was surprising since the plasma levels of most other neutrophil granule proteins are low compared to the amount in circulating neutrophils (*21*). Also, human CRISP-3 is a small (approximately 28 kDa) and positively charged protein (theoretical pI = 8.1) and is likely to be easily excreted in the urine if freely present in plasma in its monomeric form (*17*). We therefore hypothesized that CRISP-3 in human plasma was bound to another component.

In this study, we demonstrate that CRISP-3 in plasma is complex-bound to α_1B-glycoprotein (A1BG), which is a known plasma protein belonging to the immunoglobulin superfamily but with a hitherto unknown function (*22*). Furthermore, we examine the nature and stoichiometry of the complex and evaluate the capacity of CRISP-3 binding in plasma. On the basis of homology between A1BG and serum proteins from opossum species, which by complex formation inactivate toxic components in snake venom (metalloproteinases and myotoxins) (*23*−*26*), we suggest that the purpose of complex formation between CRISP-3 and A1BG is to protect the circulation from a potentially harmful effect of free CRISP-3.

EXPERIMENTAL PROCEDURES

Materials. Human plasma from EDTA anticoagulated blood was obtained from healthy volunteers. Specific anti-human CRISP-3 antiserum was generated by immunization of rabbits with a recombinant carboxy-terminally truncated form of CRISP-3 (*17*). Human A1BG and rabbit anti-human A1BG antiserum were obtained from Dade Behring (Marburg, Germany). Human serum albumin (HSA), the nondenatured protein molecular weight marker kit, and PNGase F were from Sigma. CNBr-activated Sepharose, PD-10 columns, size-exclusion standards, and columns for size-exclusion chromatography and ion-exchange chromatography were from Amersham Biosciences (Uppsala, Sweden).

Purification of CRISP-3 from Neutrophils. Native CRISP-3 was purified from isolated human neutrophils partly as previously described (*16*, *17*). Neutrophils resuspended in Krebs−Ringer phosphate solution (130 mM NaCl, 5 mM KCl, 1.27 mM $MgCl_2$, 0.95 mM $CaCl_2$, 10 mM NaH_2PO_4/Na_2HPO_4, pH 7.4, and 5 mM glucose) at a concentration of 5×10^8 cells/mL were stimulated for exocytosis with phorbol 12-myristate 13-acetate (5 μg/mL) in the presence of protease inhibitors. Following stimulation for 20 min, the cells were pelleted, and the supernatant was diluted with 1 volume of a salt- and detergent-containing buffer (1 M NaCl, 1% Triton X-100, 50 mM NaH_2PO_4/Na_2HPO_4, pH 7.4). For the initial studies, this material was applied to an affinity chromatography column with anti-CRISP-3 antibodies immobilized on CNBr-activated Sepharose. After extensive washing with buffer (0.5 M NaCl, 50 mM NaH_2PO_4/Na_2HPO_4, pH 7.4), initially supplemented with 0.5% Triton X-100, bound protein was eluted with 3 M KSCN, immediately dialyzed in phosphate-buffered saline (PBS), and finally concentrated using Centricon YM-10 (Millipore, Bedford, MA).

Following the identification of A1BG as a high-affinity binding protein, CRISP-3 for the subsequent studies was purified on an affinity chromatography column with A1BG immobilized on CNBr-activated Sepharose. After being washed as described above, bound protein was eluted with 0.2 M glycine hydrochloride (pH 2.5) and immediately neutralized with 2 M Tris-HCl (pH 9.0). This elution procedure was chosen because it proved to be more efficient and easier to handle than 3 M KSCN. The buffer was changed to 50 mM NaH_2PO_4/Na_2HPO_4, pH 6.0, using PD-10 columns, and the sample was further purified by cation-exchange chromatography on MonoS using Äkta FPLC (Amersham Biosciences). CRISP-3 eluted as two partly overlapping peaks at a plateau phase with 0.1 M NaCl and 50 mM NaH_2PO_4/Na_2HPO_4, pH 6.1. By this additional step, the CRISP-3 preparation was also concentrated and separated into two different molecular mass forms representing glycosylated and unglycosylated CRISP-3 (*17*). All procedures were performed at 4 °C, except stimulation of cells (37 °C) and cation-exchange chromatography (room temperature). CRISP-3 originating from both purification protocols was >95% pure as judged from sodium dodecyl sulfate−polyacrylamide gel electrophoresis (SDS−PAGE).

Affinity Purification of Anti-A1BG Antibodies. Rabbit anti-A1BG antiserum was diluted with 1 volume of buffer (0.5 M NaCl, 50 mM NaH_2PO_4/Na_2HPO_4, pH 7.4) and affinity purified on a separate column with A1BG immobilized on CNBr-activated Sepharose. After extensive washing with buffer, bound anti-A1BG antibodies were eluted with 3 M KSCN and immediately dialyzed in coupling buffer (0.1 M $NaHCO_3$, 0.5 M NaCl, pH 8.5). The anti-A1BG antibodies were found to retain the activity against A1BG in immunoblotting of plasma and pure A1BG. A portion of the antibodies were diluted in PBS containing 0.5% bovine

serum albumin (BSA) and 0.1% sodium azide and subsequently used for immunoblotting.

SDS−PAGE and Native PAGE. For polyacrylamide gel electrophoresis, the Mini-Protean 3 system (Bio-Rad Laboratories, Hercules, CA) was used. SDS−PAGE was performed under nonreducing conditions according to Laemmli (*27*) in 12% separating and 3% stacking gels. The same buffer system with the exclusion of SDS was used for native PAGE in 10% separating and 3% stacking gels. Gels were stained in Coomassie Brilliant Blue or used for immunoblotting.

Immunoblotting. Protein was transferred from polyacrylamide gels in 10 mM CAPS, pH 11.0, and 10% methanol using a Bio-Rad mini trans-blot module (Bio-Rad Laboratories) (*28*). Additional binding sites were blocked by incubation of the nitrocellulose blots in 5% skim milk in PBS for 1 h. The blots were incubated overnight with primary antibody, which was either anti-CRISP-3 antiserum diluted 1/1000 or affinity-purified anti-A1BG antibodies. The following day, the blots were incubated for 2 h with peroxidase-conjugated swine anti-rabbit immunoglobulins (DAKO, Glostrup, Denmark) diluted 1/1000 and developed with diaminobenzidine/metal concentrate and stable peroxide substrate buffer (Pierce, Rockford, IL).

Size-Exclusion Chromatography of Plasma. Plasma proteins were separated on the basis of molecular size by gel filtration on a Superose 12 HR 10/30 column using Äkta FPLC under different conditions. Plasma was diluted with 1 volume of buffer [either PBS (pH 7.4), 1 M NaCl in 50 mM NaH_2PO_4/Na_2HPO_4 (pH 7.4), 3 M KSCN in H_2O (pH 6.3), or 25 mM *n*-octyl β-D-glucopyranoside (NOG) in PBS (pH 7.4)], incubated for 30 min at 37 °C, and centrifuged or filtered through a 22 μm filter. Samples of 200 μL were applied to the column, which was equilibrated in the same buffer as was used for dilution of plasma. Sixty fractions of 0.5 mL were collected and analyzed for their content of albumin, lysozyme, CRISP-3, and A1BG.

Immunoprecipitation of Proteins from Plasma. The IgG fraction of anti-CRISP-3 antiserum (*17*) and affinity-purified anti-A1BG antibodies were immobilized on CNBr-activated Sepharose according to the manufacturers' instructions and packed in separate columns. Plasma was diluted with 1 volume of buffer (0.5 M NaCl, 50 mM NaH_2PO_4/Na_2HPO_4, pH 7.4) and applied to the columns. After extensive washing with buffer, initially supplemented with 0.5% Triton X-100, bound proteins were eluted with 3 M KSCN and immediately dialyzed in PBS. Subsequently, the proteins were precipitated with 5% trichloroacetic acid (TCA), washed four times in acetone, resuspended and boiled in nonreducing sample buffer, and evaluated by SDS−PAGE and immunoblotting.

Identification by Mass Spectrometry. The protein that was co-immunoprecipitated from plasma with anti-CRISP-3 antibodies was identified as described previously (*29*). In short, the relevant band was excised from the polyacrylamide gel, reduced, alkylated using iodoacetamide, and digested by trypsin. The resulting fragments were extracted, purified using C18 ZipTip (Millipore), and measured by MALDI-TOF mass spectrometry on a Biflex instrument (Bruker, Bremen, Germany).

The peptide molecular mass fingerprint was used for a search of the SWISS-PROT and TrEMBL database using the "PeptIdent" tool on the ExPaSy Molecular Biology Server of the Swiss Institute of Bioinformatics.

Complex Formation. The ability of CRISP-3 to form complexes with A1BG was examined by mixing the pure proteins in a physiological buffer (PBS), incubating for 15−30 min at 37 °C, and evaluating samples by size-exclusion chromatography and native PAGE. As a control, possible complex formation with human serum albumin (HSA), which is a major plasma protein with a p*I* (=4.7) close to the reported value for A1BG (p*I* = 4.4−4.6) (*22*), was also evaluated. For size-exclusion chromatography, samples with CRISP-3 (0.01 mg/mL ≈ 0.4 μM) and A1BG (0.1 mg/mL ≈ 1.5 μM) or HSA (0.5 mg/mL ≈ 7.5 μM), respectively, were applied to the Superose 12 column, as described above. Individual fractions were assayed for their content of the applied proteins. For native PAGE, equimolar amounts of the proteins were mixed.

In one set of experiments, equimolar amounts of CRISP-3 and A1BG were preincubated separately in the presence of 10 mM EDTA, mixed, and incubated in PBS with 10 mM EDTA, followed by evaluation on native PAGE and size-exclusion chromatography in the same buffer.

An additional experiment was performed with 3 M NaCl. Equimolar amounts of CRISP-3 and A1BG were preincubated in PBS, diluted 5-fold in 3 M NaCl and 50 mM NaH_2PO_4/Na_2HPO_4, pH 7.4, and subjected to size-exclusion chromatography in the same buffer.

Surface Plasmon Resonance Analysis of Binding Kinetics. Kinetic measurements of the interaction between CRISP-3 and A1BG were performed by real-time interaction analysis using a BIAcore 2000 instrument (Biacore, Uppsala, Sweden). The two naturally occurring forms of CRISP-3 (i.e., glycosylated 29 kDa and unglycosylated 27 kDa protein) were separately diluted (final concentration 200 nM) in 10 mM acetate buffer (pH 5.26) and immobilized via amine coupling on a CM5-type sensor chip using 0.2 M *N*-ethyl-*N*′-(3-dimethylaminopropyl)carbodiimide (EDC) and 0.05 M *N*-hydroxysuccinimide (NHS) according to the procedure described by the manufacturer. After the protein was coupled, excessive reactive sites were blocked with 1 M ethanolamine. Binding analyses were performed using HEPES-buffered saline (HBS; 10 mM HEPES, pH 7.4, 150 mM NaCl, 0.005% surfactant P20, and 3 mM EDTA) as running buffer at 11 or 25 °C. Thirty-five microliters of varying concentrations of A1BG (10−400 nM) in HBS was injected in repetitive cycles. Association was monitored during a 3.5 min injection phase. Dissociation was monitored during 3 min after return to buffer flow. Regeneration of the sensor chip was achieved by a pulse injection of 10 mM glycine hydrochloride between each cycle. All interaction analyses were performed at a continuous flow rate of 10 μL/min. Sensorgrams obtained from a parallel flow cell, coupled in the presence of HBS only, served as blanks allowing subtraction of the bulk.

To determine the kinetic binding constants (k_a, k_d, and the derived K_D), the binding data were analyzed by nonlinear regression (*30*) using BIAevaluation 3.0 software assuming a 1:1 binding model.

Stoichiometry of the Complex. A fixed amount of CRISP-3 (mixture of glycosylated and unglycosylated) was incubated with A1BG at different molar ratios (A1BG/CRISP-3 at 0.2:1 to 3.2:1), and 200 μL samples were subjected to size-exclusion chromatography on a Superose 6 HR 10/30 column

using Äkta FPLC. As controls, samples of pure CRISP-3 and A1BG alone were subjected to the same procedure. The incubation and running buffer was PBS, pH 7.4. Fractions of 0.25 mL were collected and assayed for their content of the individual proteins by ELISAs and polyacrylamide gel electrophoresis. Chromatograms were analyzed using Unicorn 3.10 software (Amersham Biosciences).

Amino Acid Sequencing. Equimolar amounts of CRISP-3 and A1BG were incubated together, separated by native PAGE, and transferred to a PVDF membrane, as described above. After being stained in Amido Black, the band representing the A1BG−CRISP-3 complex was excised and subjected to N-terminal sequence analysis in a 494A Procise protein sequencer (Perkin-Elmer, Palo Alto, CA), as described previously (*29*).

Deglycosylation of A1BG. A sample of A1BG was deglycosylated with PNGase F as described by the manufacturer, except that denaturing agents and heating were omitted. In short, 25 μg of A1BG was diluted in PBS supplemented with 0.7% Triton X-100. After addition of enzyme, the sample was incubated at 37 °C for 26 h. Aliquots were drawn at different time points and subjected to SDS−PAGE to follow the reaction. Total deglycosylation was obtained after 24 h.

Completely deglycosylated A1BG was mixed with equimolar amounts of CRISP-3, and the ability of complex formation was evaluated on native PAGE and by size-exclusion chromatography on Superose 6, as described above.

Capacity of CRISP-3 Binding in Plasma. Samples of plasma with a known content of CRISP-3 (approximately 5 μg/mL) were diluted in PBS alone or supplemented with pure CRISP-3 to a total concentration of approximately 200 μg of CRISP-3/mL of plasma. The samples were subsequently subjected to size-exclusion chromatography on Superose 6, as described above, except that fractions of 0.5 mL were collected. The fractions were assayed for their content of CRISP-3 and A1BG.

Quantification of Proteins. The concentration of pure protein samples was determined spectrophotometrically using molar extinction coefficients at 280 nm for CRISP-3 (55580 M^{-1} cm^{-1}) and A1BG (53230 M^{-1} cm^{-1}), estimated as described (*31*).

The concentration of individual proteins in mixed samples was measured by ELISAs. Albumin and lysozyme were assayed by standard sandwich ELISAs described in refs *32* and *33*. CRISP-3 was analyzed using a modified sandwich ELISA, in which samples are denatured by pretreatment with SDS and dithiothreitol (*17*). A1BG was measured by a semiquantitative ELISA almost identical to the procedures described by Sørensen et al. (*21*), except that anti-A1BG antiserum (diluted 1/1000) was used for detection.

Determination of Molecular Mass. To estimate the molecular mass of individual proteins and complexes, Ferguson plot analysis was performed with a series of 5−10% native gels (*34*). The relative mobilities of α-lactalbumin (14.2 kDa), carbonic anhydrase (29.2 kDa), ovalbumin (45 kDa), BSA (monomer, 66 kDa; dimer, 132 kDa), and urease (trimer, 272 kDa; hexamer, 545 kDa) were determined following Coomassie Blue staining and normalized to the dye front. The relative mobility of A1BG and the A1BG−CRISP-3 complex was determined on the same gels, and apparent molecular masses were determined from the plot.

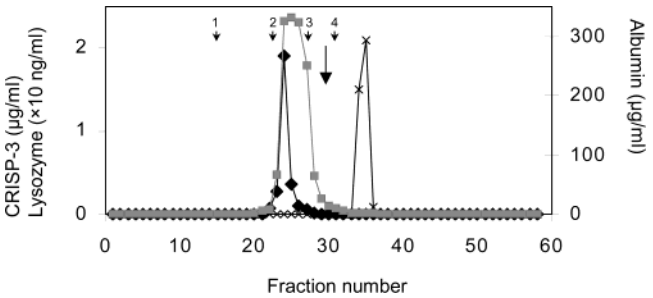

FIGURE 1: Size-exclusion chromatography of plasma. Plasma proteins were separated on a Superose 12 column equilibrated in PBS. The concentration of CRISP-3 (◆), albumin (■), and lysozyme (×) was measured in each fraction using ELISAs. The long arrow indicates the expected peak elution volume of free monomeric CRISP-3. Small arrows indicate the elution volume of calibrators [1, blue dextran (void volume); 2, BSA dimer (132 kDa); 3, ovalbumin (45 kDa); and 4, chymotrypsinogen (25 kDa)].

Molecular masses were also estimated by size-exclusion chromatography on both the Superose 6 and Superose 12 column. Size-exclusion standards in PBS (aldolase, 158 kDa, BSA monomer and dimer, ovalbumin, chymotrypsinogen A, 25 kDa, and ribonuclease A, 13.7 kDa) were examined using the same sample size and flow as in the experiments described above. Elution volumes were determined from the chromatograms and used to construct the calibration curves.

Linear regression analyses were performed using the SAS System for Windows V8. Apparent molecular masses were calculated from the derived formulas.

RESULTS

Identification of A1BG as a Binding Partner of CRISP-3 in Plasma. We have previously demonstrated the presence of CRISP-3 in human plasma by ELISA and immunoblotting, and both the glycosylated (29 kDa) and unglycosylated (27 kDa) forms were found, identical to CRISP-3 from neutrophils (*17*). Because of the unexpected high concentration of CRISP-3, we hypothesized that CRISP-3 in plasma behaves as a larger protein possibly by complex formation with another component. To elucidate this, we performed size-exclusion chromatography of plasma under physiological conditions on a Superose 12 column and measured the content of specific proteins in eluted fractions. The elution profiles of CRISP-3, albumin, and lysozyme are shown in Figure 1 and demonstrate that CRISP-3 eluted in a single peak one fraction earlier than albumin, corresponding to a molecular mass of about 100 kDa. In previous studies with purification of CRISP-3 from neutrophils (*17*), we found CRISP-3 in fractions corresponding to its own monomeric size (25−30 kDa), indicating that CRISP-3 does not form homodimers or homotrimers in solution.

To identify a potential binding partner of CRISP-3, we immunoprecipitated CRISP-3 from plasma using specific anti-human CRISP-3 antibodies raised against a recombinant form of CRISP-3. When the TCA-precipitated eluate was examined by SDS−PAGE (see Figure 2A), a major band with an apparent size of 75−80 kDa was observed in addition to the two bands representing CRISP-3. The size of the coprecipitated protein was in agreement with the expected size from the size-exclusion chromatography of plasma. The band was excised from the gel, and tryptic fragments were analyzed by mass spectrometry. A database search with this

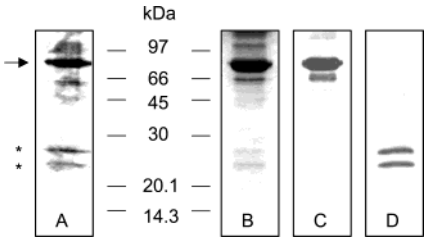

FIGURE 2: Immunoprecipitation of CRISP-3 and A1BG from plasma. Plasma was loaded on columns with immobilized anti-CRISP-3 antibodies (A) or affinity-purified anti-A1BG antibodies (B−D). The eluates were TCA-precipitated and analyzed by 12% SDS−PAGE. (A, B) Gels stained in Coomassie Brilliant Blue; (C) immunoblotting using affinity-purified anti-A1BG antibodies; (D) immunoblotting using anti-CRISP-3 antiserum [a double amount of sample was applied on the gel compared to (B) and (C)]. The position of the two forms of CRISP-3 on the gel is indicated (*). The arrow indicates the potential binding partner of CRISP-3.

Table 1: Identification of Coprecipitated A1BG by Mass Spectrometry of Tryptic Fragments

fragment[a]	molecular mass (Da)[b] experimental	theoretical
32−41	1237.69	1237.65
42−57	nd	1674.88
58−69	1372.76	1372.70
74−85	1264.72	1264.65
86−93	870.52	870.53
94−113	2151.22	2151.17
124−130	805.47	805.49
207−223	1876.08	1876.00
241−259	2148.16	2148.04
304−312	986.50	986.51
371−385	1724.02	1723.96
386−396	1088.61	1088.59
402−415	1645.89	1645.83
427−448	2296.33	2296.18
453−474	2471.37	2471.20

[a] All expected fragments with a molecular mass between 800 and 2500 Da are listed (in accordance with ref *22*, where amino acid residues in the mature chain are numbered 1−474). [b] Molecular masses are given as monoisotopic values for the $M + H^+$ ion determined by MALDI-TOF MS. nd = not detected.

set of molecular masses identified human α_1B-glycoprotein (A1BG) with a high score, covering 42% of the sequence distributed among 14 peptides with molecular masses matching the theoretical values within 70 ppm, as shown in Table 1. Since this protein is a well-known component of plasma and the reported size in SDS−PAGE of 80 kDa (*22*) was consistent with our finding, we attempted to prove that this protein was responsible for the complex binding of CRISP-3. We established a semiquantitative ELISA for A1BG and measured the content in fractions from the size-exclusion chromatography of plasma described above. The elution profile of A1BG showed a single peak totally overlapping the elution profile of CRISP-3 (not shown). When the pure proteins were mixed and incubated in a physiological buffer followed by size-exclusion chromatography, CRISP-3 and A1BG coeluted as shown in Figure 3A. To ensure that this was not merely a result of weak interactions between proteins of opposite charges, the same experiment was performed with CRISP-3 and albumin, since albumin has about the same charge as A1BG (experimental p*I* close to 4.6 for both). As shown in Figure 3B, CRISP-3 and albumin eluted in two separate peaks. The same ability of complex formation was observed, when equimolar mixtures were analyzed on

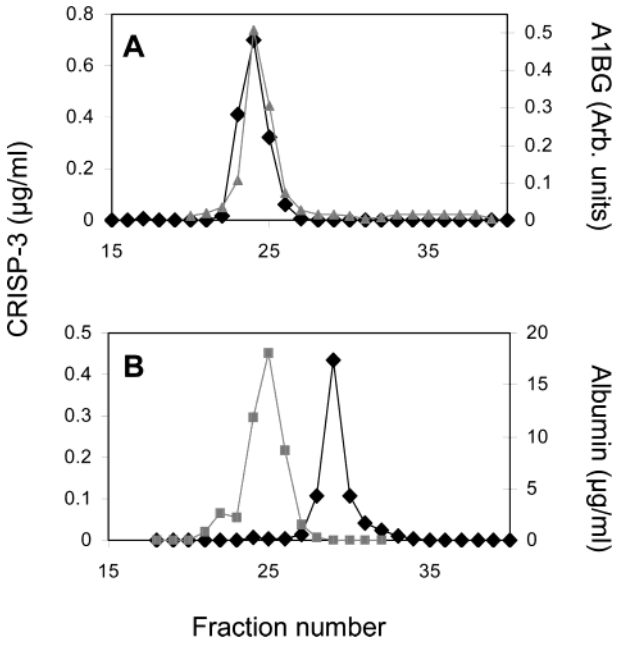

FIGURE 3: Size-exclusion chromatography of CRISP-3 preincubated with A1BG or albumin. Samples of pure CRISP-3 and A1BG (A) or albumin (B), respectively, were incubated at 37 °C and subsequently separated on a Superose 12 column equilibrated in PBS. The concentration of CRISP-3 (◆), A1BG (▲), and albumin (■) was measured in relevant fractions using ELISAs.

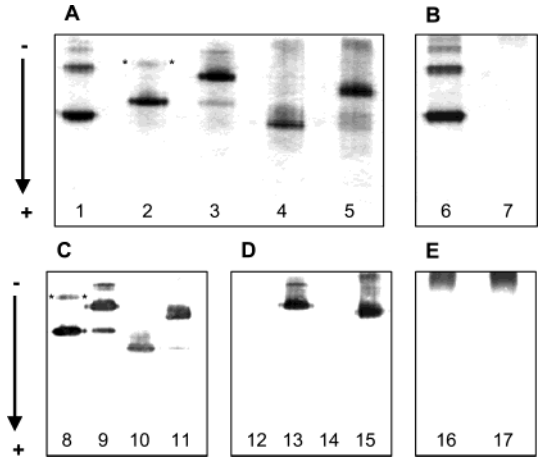

FIGURE 4: Complex formation between CRISP-3 and A1BG before and after deglycosylation. Natural (i.e., fully glycosylated) and deglycosylated A1BG were incubated with equimolar amounts of CRISP-3 and analyzed by native PAGE (10%) (A, C, D). Possible complex formation between HSA and CRISP-3 was also evaluated (B, E). (A, B) Gels stained in Coomassie Brilliant Blue; (C) immunoblotting using affinity-purified anti-A1BG antibodies; (D, E) immunoblotting using anti-CRISP-3 antiserum. Lanes: 1, human serum albumin (both monomer and dimer are seen); 2, 8, and 12, natural A1BG [the band indicated (*) is likely to represent A1BG dimer]; 3, 9, and 13, natural A1BG incubated with CRISP-3 (the dominant band represents the A1BG−CRISP-3 complex, whereas the upper faint band is likely to represent double complexes; the lower faint band in lanes 3 and 9 represents free A1BG); 4, 10, and 14, deglycosylated A1BG; 5, 11, and 15, deglycosylated A1BG incubated with CRISP-3; 6 and 16, HSA incubated with CRISP-3 (no complex formation is seen); 7 and 17, CRISP-3 alone. The band in the top of the gels (lanes 6, 7, and 15−17) is likely to represent free CRISP-3, which is almost uncharged at the pH used and does not run into the gel.

native PAGE (Figure 4, lanes 1−3 and 6). Finally, A1BG was immunoprecipitated from plasma using affinity-purified anti-A1BG antibodies and now the two forms of CRISP-3

were coprecipitated (Figure 2B−D).

Characterization of the A1BG−CRISP-3 Complex. From a prior study (*17*), we knew that CRISP-3 is not covalently attached to another component, since separation of plasma proteins by SDS−PAGE followed by immunoblotting for CRISP-3 resulted in two bands according to the expected sizes even under nonreducing conditions, where only noncovalent bonds are dissociated. To evaluate the nature of the binding between CRISP-3 and A1BG, size-exclusion chromatographies of plasma proteins were repeated using buffers with different ionic strength and hydrophobic properties (1 M NaCl, 3 M KSCN, and 25 mM NOG, respectively). Only the buffer with the highest ionic strength but also chaotropic properties, i.e., 3 M KSCN, was capable of dissociating the complex, resulting in elution of CRISP-3 according to its molecular mass, whereas the elution profile was unchanged in the buffer with nonionic detergent (NOG) (not shown). This indicated that disruption of hydrophobic interactions alone was insufficient to dissociate the complex. Because size-exclusion chromatography of plasma was incompatible with 3 M NaCl, the complex alone was evaluated in this buffer. Here the two proteins eluted together (not shown), indicating that dissociation of the complex was not accomplished even by such high ionic strength. However, during optimization of the purification protocol for CRISP-3, low pH proved to be superior to 3 M KSCN in disrupting the A1BG−CRISP-3 complex. Together, these observations indicate that the complex is primarily dependent on strong electrostatic forces or maybe on steric complementarity since low pH (like 1% SDS and 3 M KSCN) also has a denaturing effect disturbing the tertiary structure of the proteins.

A1BG has been reported to have a 13.3% carbohydrate content due to four N-glycosylation sites in the amino acid sequence (*22*). To investigate whether this glycosylation is necessary for complex formation with CRISP-3, a sample of A1BG was deglycosylated using PNGase F, which completely removes asparagine-linked oligosaccharides from glycoproteins. When deglycosylated A1BG was incubated with CRISP-3 and subsequently analyzed by native PAGE (Figure 4A,C,D) and size-exclusion chromatography, it was observed that complex formation was not hindered. However, a portion of the deglycosylated A1BG (but no CRISP-3) eluted in the void volume in size-exclusion chromatography (not shown), probably as a result of aggregation because no detergent was included in the chromatography buffer. A similar tendency to aggregate in aqueous solution has previously been reported for the homologous proteins DM40 and DM43 following chemical deglycosylation (*35*) and indicates that glycosylation is important for other purposes.

We also examined if complex formation was dependent on Ca^{2+} or other divalent metal ions by including the chelating agent EDTA in buffers. Under this condition, full complex formation was still observed both by native PAGE and by size-exclusion chromatography, and no change in mobility or elution profile was found (not shown, but figures would be identical to Figure 4, lanes 2 and 3, and Figure 7A).

The apparent high affinity between CRISP-3 and A1BG observed in the binding experiments and from purification of CRISP-3 using A1BG immobilized on CNBr−Sepharose was further examined by continuous monitoring of binding and dissociation provided by BIAcore technology. The affinity was evaluated separately for the two forms of CRISP-3 found in plasma. The sensorgrams in Figure 5 show that injection of A1BG onto immobilized CRISP-3 gave significant responses with fast association and slow dissociation phases, as expected. The calculated kinetic binding parameters are shown in Table 2, and it is seen that the apparent equilibrium dissociation constant (K_D) is of the same order of magnitude for both glycosylated and unglycosylated CRISP-3. The low K_D in the nanomolar range indicates that the two forms of CRISP-3 have equal and high affinity toward A1BG.

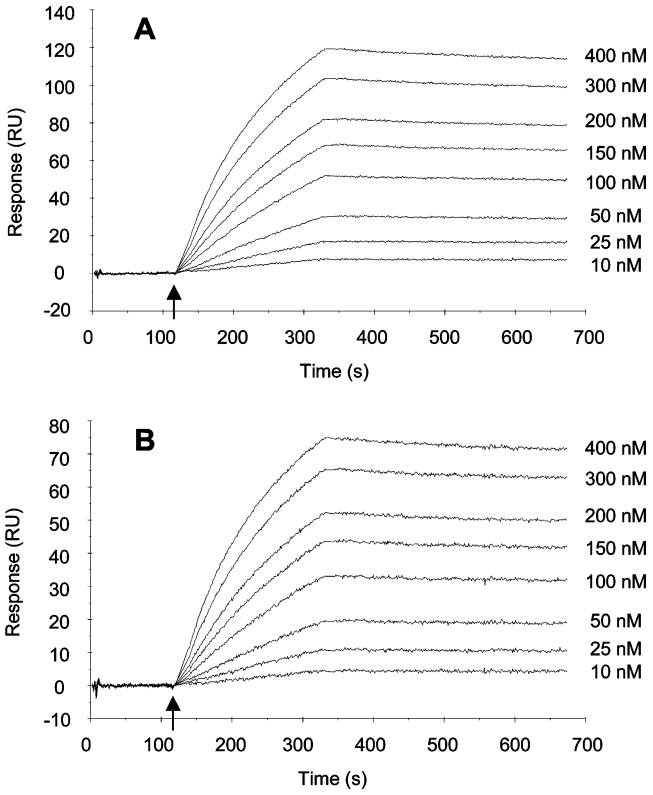

FIGURE 5: Sensorgrams for the interaction between A1BG and immobilized CRISP-3 measured by surface plasmon resonance. Glycosylated (A) and unglycosylated (B) CRISP-3 were coupled onto a CM5-type sensor chip at levels of 776 and 444 resonance units (RU), respectively. Sensorgrams were obtained from injections of A1BG at different concentrations ranging from 10 to 400 nM at a flow rate of 10 μL/min. Subtraction of background and fitting of the curves were performed using BIAevaluation 3.0 software. Overlayed sensorgrams obtained at 11 °C are shown. The arrows indicate start of injection.

Table 2: Kinetic Parameters for the Interaction between A1BG and CRISP-3[a]

CRISP-3	temp (°C)	k_a (M^{-1} s^{-1})	k_d (s^{-1})	K_D (nM)
glycosylated	25	$(7.69 \pm 3.0) \times 10^4$	$(1.63 \pm 0.1) \times 10^{-4}$	2.1
(29 kDa)	11	$(3.27 \pm 1.7) \times 10^4$	$(1.34 \pm 0.2) \times 10^{-4}$	4.1
unglycosylated	25	$(7.50 \pm 2.4) \times 10^4$	$(2.09 \pm 0.7) \times 10^{-4}$	2.8
(27 kDa)	11	$(3.26 \pm 1.7) \times 10^4$	$(1.39 \pm 0.4) \times 10^{-4}$	4.3

[a] Kinetic parameters were derived from BIA sensorgrams recording the association and dissociation of various A1BG concentrations with the respective forms of immobilized CRISP-3 at two different temperatures. Rate constants for association (k_a) and dissociation (k_d) are expressed as the mean of the apparent values for eight different A1BG concentrations (10−400 nM). The standard deviations are indicated. The apparent equilibrium dissociation constant (K_D) was calculated from the experimentally determined k_a and k_d as k_d/k_a.

Table 3: Molecular Masses Determined by Different Methods[a]

	native PAGE	Superose 6	Superose 12
CRISP-3	nd	24	23
A1BG	74	91	82
A1BG−CRISP-3	99	107	102
A1BG dimer	163	204	157

[a] Molecular masses of individual proteins and complexes were estimated by native PAGE using a Ferguson plot and by size-exclusion chromatography on a Superose 6 and a Superose 12 column, as described in Experimental Procedures. Molecular masses are expressed in kDa. nd = not determined.

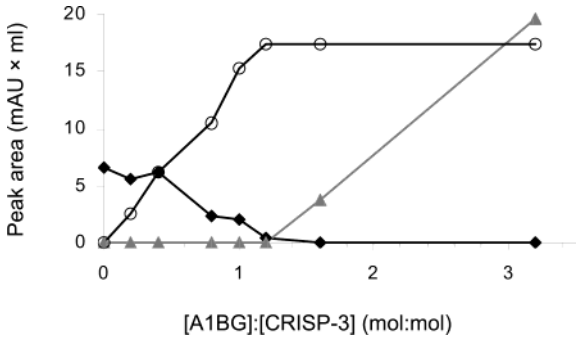

FIGURE 6: Titration of CRISP-3 with A1BG. A fixed amount of CRISP-3 was mixed with increasing amounts of A1BG and incubated at 37 °C in PBS. The samples were subjected to size-exclusion chromatography on a Superose 6 column. At each molar ratio, peak areas corresponding to free CRISP-3 (◆), free A1BG (▲), and the A1BG−CRISP-3 complex (○) were integrated and plotted. mAU = milli-absorbance units (280 nM). Selected chromatograms are shown in Figure 7.

Stoichiometry of the A1BG−CRISP-3 Complex. The results from estimation of the molecular masses of CRISP-3, A1BG, and the complex by native PAGE and size-exclusion chromatography are shown in Table 3. The majority of A1BG behaved as a protein with an apparent mass corresponding to the expected monomeric form, whereas a minor portion behaved as a protein with a mass corresponding to a dimer. From Figure 4 (lanes 8 and 9 and 12 and 13) it is obvious that both forms react with the anti-A1BG antibody and bind CRISP-3. We can thus conclude that pure A1BG in solution, like HSA (Figure 4, lanes 1 and 2), predominantly exists as a monomer and a few percent as a dimer. The estimated mass of the prevalent A1BG−CRISP-3 complex (Table 3) is in agreement with a 1:1 stoichiometry of the complex. Also, analysis of the kinetic parameters (BIAcore) fitted well with this model. However, A1BG is known to have five immunoglobulin domains (*22*) and binding of more than one CRISP-3 molecule per A1BG molecule cannot be excluded on the basis of these experiments alone, since binding of an additional CRISP-3 molecule per complex would only increase the mass with 25% and at the same time would change the overall charge and conformation. To determine the stoichiometry, a titration assay was performed with a series of size-exclusion chromatographies with different molar ratios of the two proteins. A fixed amount of CRISP-3 was mixed with increasing amounts of A1BG, and the quantity of free CRISP-3, free A1BG, and the A1BG−CRISP-3 complex was determined from the chromatograms (*24*, *26*). The results in Figure 6 show that as long as the molar concentration of CRISP-3 exceeded the concentration of A1BG (molar ratio < 1), free CRISP-3 was still present. When the molar concentration of A1BG was higher than the

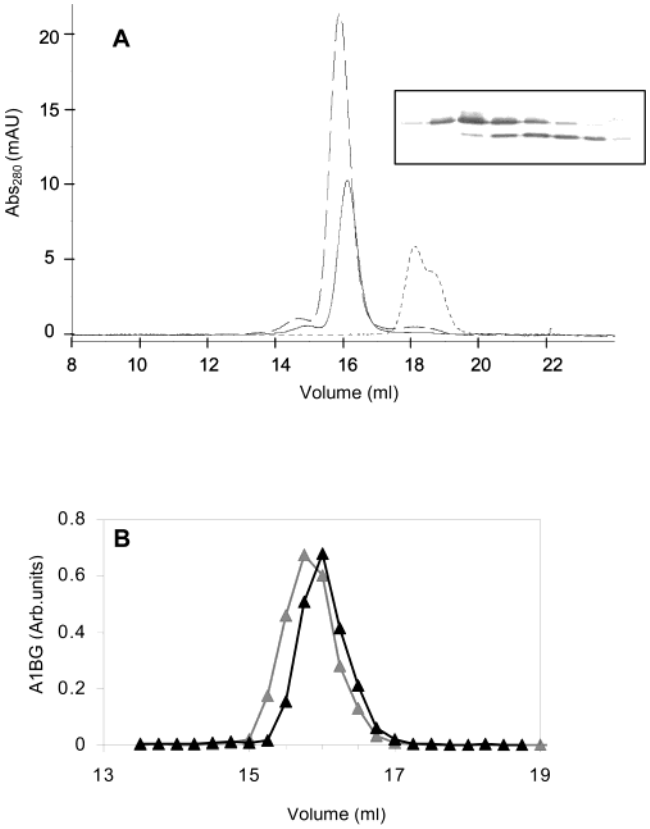

FIGURE 7: Complex formation between A1BG and CRISP-3. (A) Overlayed chromatograms from three different size-exclusion chromatographies with CRISP-3 alone (---), A1BG alone (—), and the A1BG−CRISP-3 complex (— —), formed by a nearly equimolar ratio (1.2:1). Results derived from the chromatograms are also included in Figure 6. Inset: Immunoblotting of fractions corresponding to the CRISP-3 peak, displaying the separation of glycosylated and unglycosylated protein. (B) Overlayed A1BG ELISA profiles from two size-exclusion chromatographies with A1BG alone (▲) and A1BG−CRISP-3 at a nearly equimolar ratio (1.2:1) (gray ▲).

concentration of CRISP-3 (molar ratio > 1.2), free CRISP-3 was absent, and a saturable amount of complex was formed. This clearly indicated interaction of one molecule of CRISP-3 with one molecule of A1BG. If one A1BG molecule could bind two or more CRISP-3 molecules, one would expect free CRISP-3 to be absent already at lower ratios. In Figure 7A showing overlayed chromatograms from three different chromatographies (A1BG alone, CRISP-3 alone, and fully complex formation, respectively) and Figure 7B showing the A1BG ELISA profiles, it is seen that the complex peaks approximately 0.25 mL before free A1BG [95% confidence intervals using Student's *t*-test (two-sided) = 0.211−0.263 mL; $n = 6$]. The same is the case with the small peaks to the left, which are likely to represent the A1BG dimer and double complex (2:2), respectively. When a large excess of A1BG was present, the chromatographic profile representing the sum of complex and free A1BG was shifted back to the position of the profile representing free A1BG, and the relative size of the small peak representing dimers was not increased (not shown). This is also totally in line with the suggested stoichiometry and furthermore excludes the possibility that one CRISP-3 molecule could bind two A1BG molecules. In Figure 7A it is also observed that the chromatographic profile of free CRISP-3 is a broad peak with a "shoulder" to the right, which is caused by the mix-

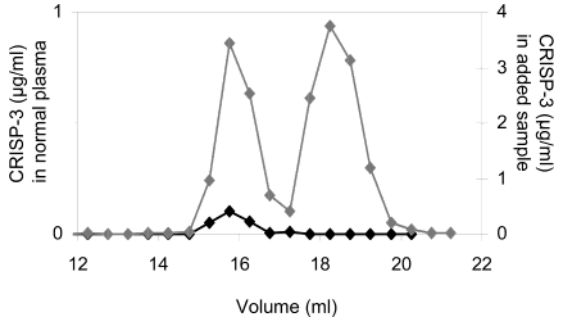

FIGURE 8: Capacity of CRISP-3 binding in plasma. Plasma samples of 25 μL were diluted in PBS alone (◆) or supplemented with pure CRISP-3 to a total concentration of 200 μg/mL of plasma (gray ◆) and subsequently separated on a Superose 6 column. Samples of 200 μL were applied. The concentration of CRISP-3 was measured in relevant fractions by ELISA.

ture of 29 and 27 kDa CRISP-3 used in the experiments (shown in inset). The CRISP-3 peak retained this morphology in all of the chromatographies, where free CRISP-3 was present (not shown), which also indicates that the two forms of CRISP-3 have equal affinity for A1BG. The conclusions drawn from the chromatograms were further substantiated by evaluating the content of A1BG and CRISP-3 in the eluted fractions by ELISA and SDS−PAGE (partly shown in Figure 7).

Finally, the quantitative relation between CRISP-3 and A1BG was estimated from amino-terminal protein sequence analysis of a PVDF membrane blot of the complex from a native PAGE purification. The first 20 residues were analyzed, and two parallel sequences were identified, corresponding to the amino termini of CRISP-3 and A1BG, respectively. The initial yields of the two proteins were very similar as estimated from the extrapolation of the combined repetitive yields to "residue 0", being 22 and 25 pmol, respectively. Furthermore, the response from identical residues not too far apart in the two proteins was very similar when allowing for the falling yield through the sequence analysis [Glu-2 (19 pmol), Pro-6 (16 pmol), and Thr-9 (16 pmol) of CRISP-3 compared to Glu-5 (16 pmol), Pro-8 (12 pmol), and Thr-6 (20 pmol) of A1BG].

Capacity of CRISP-3 Binding in Plasma. The reported concentration of A1BG in plasma from normal adults is about 220 μg/mL and the molecular weight 68000 (*22*), giving a molar concentration of 3.2 μM. With the suggested 1:1 stoichiometry of the A1BG−CRISP-3 complex, we would expect A1BG to have a binding capacity for an equimolar amount of CRISP-3 (or approximately 90 μg of CRISP-3/mL of plasma, assuming a mean molecular weight of CRISP-3 of 28000) if A1BG does not bind other agents. From the immunoprecipitation of A1BG from plasma (Figure 2B), other high-affinity ligands were not observed, and most of the A1BG seemed to be unsaturated with ligand. To test the hypothesis, we performed size-exclusion chromatography of a plasma sample with a known content of CRISP-3 (5 μg/mL $\approx$ 0.2 μM) with the addition of pure CRISP-3 from neutrophils to a total concentration of 200 μg of CRISP-3/mL of plasma ($\approx$7 μM). The content of CRISP-3 was measured in individual fractions, and the results shown in Figure 8 demonstrate that almost half of the CRISP-3 eluted in the fractions corresponding to the complex, as expected.

DISCUSSION

Human A1BG has been known for four decades (*36*), and the amino acid sequence (single polypeptide chain of 474 amino acids), chromosomal assignment (chromosome 19), and genetic polymorphism in different populations were described during the 1980s (*22*, *37*, *38*). Despite this, no influence of various diseases on the plasma level has been reported, and no biological function has been suggested. Computer analysis of the sequence showed A1BG to consist of five repeating structural domains, each corresponding to a variable domain in immunoglobulins (*22*, *39*). A1BG is thus a member of the immunoglobulin superfamily, which serves diverse functions based on molecular recognition especially in the immune system and in cell adhesion (*39*).

Human CRISP-3 was first described in 1996 (*1*, *2*), and the abundant presence in plasma was demonstrated in 2002 (*17*). In our search for a binding partner of CRISP-3 in plasma, we have identified CRISP-3 as a specific ligand of A1BG, and this is the first study to suggest a function for A1BG. Our results demonstrate that A1BG with high affinity forms stable, noncovalent, 1:1 stoichiometric complexes with CRISP-3 and thus prevents the existence of free CRISP-3 in plasma. Similar complexes have been described in opossum species between plasma proteins with sequence homology to A1BG (oprin, DM40, DM43, DM64, and PO41) and toxic proteins (metalloproteinases and myotoxins) from snake venom. In these cases, complex formation quickly neutralizes the toxins and protects the animals from the effect of envenomation (*23*−*26*, *35*). CRISP-3, however, has no sequence similarity to these toxins but is closely related to the neurotoxin-like CRISPs (about 50% sequence identity) also present in snake venom (*7*, *12*). It is thus likely that also human CRISP-3 possesses a toxic activity, which is meant to serve a physiological function locally (e.g., when exocytosed from neutrophilic granulocytes during migration), but is undesirable in the circulation. We therefore suggest that the function of A1BG is to bind CRISP-3 and thereby inhibit a potentially harmful effect in the circulation. The high affinity between A1BG and CRISP-3 together with the large overcapacity for CRISP-3 binding in plasma is in line with this suggestion as it secures that any CRISP-3 molecule entering the circulation can be complex-bound immediately.

The described A1BG-like proteins from opossums can be divided into two groups based on size and type of ligand. The largest group (DM40, DM43, PO41, and oprin) comprises proteins with three immunoglobulin domains and neutralizes snake venom metalloproteinases (SVMP) (*23*, *24*, *26*, *35*), whereas the other group (represented only by DM64) has five immunoglobulin domains and binds myotoxins (*25*). Because the binding between DM43 and SVMPs was shown to be dependent on an intact metalloproteinase domain (*24*) and proteins such as CRISP-3 were suggested to be metalloproteins due to a potential metal binding site in the SCP domain (*9*, *10*), we investigated if calcium or divalent metal ions were necessary for formation of the A1BG−CRISP-3 complex. This was, however, not the case since the complex was formed even in the presence of the chelating agent EDTA, as described in the Results section. This finding is also in agreement with the fact that A1BG both in domain number and in sequence has higher similarity to DM64 (37%

sequence identity), which does not bind SVMPs (*25*). Although the three most amino-terminal domains in DM64 are homologous to the three domains of DM43, a gap of four amino acids is found in the third domain of DM64 (and A1BG) in a region which in DM43 was predicted to be part of the metalloproteinase recognition site (*24*, *25*).

The A1BG-like proteins PO41, DM43, and DM64 seem to exist as homodimers, which dissociate and form heterodimers upon complex formation (*24*−*26*). In contrast to this, A1BG predominantly exists in monomeric form although a few percent was found in dimeric form, when pure protein was examined (Figures 4A,C and 7A). In all cases, however, noncovalent complexes with a 1:1 stoichiometry are formed.

Besides in humans, A1BG has also been detected in more than 40 other mammalian species and is thought to be present in plasma of all mammals (*40*). CRISP-3, however, has only been detected in three mammalian species (human, horse, and mouse) and in plasma so far only in humans. The individual A1BG-like proteins, described above, are capable of binding different ligands belonging to the same group; i.e., DM43 can bind both jararhagin and bothrolysin, which are representatives of different subgroups of SVMPs, and DM64 binds both myotoxins I and II (*24*, *25*). According to this, we would also expect A1BGs to bind different CRISPs. This idea is supported by an observation from our laboratory which indicated that human CRISP-3 was bound by nonhuman A1BG present in calf serum. The physiological implications of this observation are uncertain, but it should be taken into account when the function of CRISPs is examined in serum-containing medium.

In summary, CRISP-3 is a specific ligand of A1BG in human plasma and high-affinity, 1:1 stoichiometric complexes are formed between the two proteins. Complex formation is independent of glycosylation of either protein and also of calcium or divalent metal ions. An overcapacity of CRISP-3 binding prevents the existence of free CRISP-3 in plasma and possibly protects the circulation from a potential harmful effect. Our findings suggest a function of A1BG and add to the understanding of CRISP-3 function.

ACKNOWLEDGMENT

We thank Allan Kastrup for expert technical assistance with mass spectrometry and amino-terminal amino acid sequencing.

REFERENCES

1. Kjeldsen, L., Cowland, J. B., Johnsen, A. H., and Borregaard, N. (1996) SGP28, a novel matrix glycoprotein in specific granules of human neutrophils with similarity to a human testis-specific gene product and a rodent sperm-coating glycoprotein, *FEBS Lett. 380*, 246−250.
2. Krätzschmar, J., Haendler, B., Eberspaecher, U., Roosterman, D., Donner, P., and Schleuning, W. D. (1996) The human cysteine-rich secretory protein (CRISP) family. Primary structure and tissue distribution of CRISP-1, CRISP-2 and CRISP-3, *Eur. J. Biochem. 236*, 827−836.
3. Eberspaecher, U., Roosterman, D., Krätzschmar, J., Haendler, B., Habenicht, U. F., Becker, A., Quensel, C., Petri, T., Schleuning, W. D., and Donner, P. (1995) Mouse androgen-dependent epididymal glycoprotein CRISP-1 (DE/AEG): isolation, biochemical characterization, and expression in recombinant form, *Mol. Reprod. Dev. 42*, 157−172.
4. Haendler, B., Habenicht, U. F., Schwidetzky, U., Schuttke, I., and Schleuning, W. D. (1997) Differential androgen regulation of the murine genes for cysteine-rich secretory proteins (CRISP), *Eur. J. Biochem. 250*, 440−446.
5. Schambony, A., Gentzel, M., Wolfes, H., Raida, M., Neumann, U., and Topfer-Petersen, E. (1998) Equine CRISP-3: primary structure and expression in the male genital tract, *Biochim. Biophys. Acta 1387*, 206−216.
6. Morrissette, J., Krätzschmar, J., Haendler, B., el Hayek, R., Mochca-Morales, J., Martin, B. M., Patel, J. R., Moss, R. L., Schleuning, W. D., and Coronado, R. (1995) Primary structure and properties of helothermine, a peptide toxin that blocks ryanodine receptors, *Biophys. J. 68*, 2280−2288.
7. Yamazaki, Y., Koike, H., Sugiyama, Y., Motoyoshi, K., Wada, T., Hishinuma, S., Mita, M., and Morita, T. (2002) Cloning and characterization of novel snake venom proteins that block smooth muscle contraction, *Eur. J. Biochem. 269*, 2708−2715.
8. Fernandez, C., Szyperski, T., Bruyere, T., Ramage, P., Mosinger, E., and Wuthrich, K. (1997) NMR solution structure of the pathogenesis-related protein P14a, *J. Mol. Biol. 266*, 576−593.
9. Henriksen, A., King, T. P., Mirza, O., Monsalve, R. I., Meno, K., Ipsen, H., Larsen, J. N., Gajhede, M., and Spangfort, M. D. (2001) Major venom allergen of yellow jackets, Ves v 5: structural characterization of a pathogenesis-related protein superfamily, *Proteins 45*, 438−448.
10. Szyperski, T., Fernandez, C., Mumenthaler, C., and Wuthrich, K. (1998) Structure comparison of human glioma pathogenesis-related protein GliPR and the plant pathogenesis-related protein P14a indicates a functional link between the human immune system and a plant defense system, *Proc. Natl. Acad. Sci. U.S.A. 95*, 2262−2266.
11. Niderman, T., Genetet, I., Bruyere, T., Gees, R., Stintzi, A., Legrand, M., Fritig, B., and Mosinger, E. (1995) Pathogenesis-related PR-1 proteins are antifungal. Isolation and characterization of three 14-kilodalton proteins of tomato and of a basic PR-1 of tobacco with inhibitory activity against Phytophthora infestans, *Plant Physiol. 108*, 17−27.
12. Yamazaki, Y., Brown, R. L., and Morita, T. (2002) Purification and cloning of toxins from elapid venoms that target cyclic nucleotide-gated ion channels, *Biochemistry 41*, 11331−11337.
13. Cohen, D. J., Ellerman, D. A., Busso, D., Morgenfeld, M. M., Piazza, A. D., Hayashi, M., Young, E. T., Kasahara, M., and Cuasnicu, P. S. (2001) Evidence that human epididymal protein arp plays a role in gamete fusion through complementary sites on the surface of the human egg, *Biol. Reprod. 65*, 1000−1005.
14. Maeda, T., Nishida, J., and Nakanishi, Y. (1999) Expression pattern, subcellular localization and structure−function relationship of rat Tpx-1, a spermatogenic cell adhesion molecule responsible for association with Sertoli cells, *Dev. Growth Differ. 41*, 715−722.
15. Haendler, B., Krätzschmar, J., Theuring, F., and Schleuning, W. D. (1993) Transcripts for cysteine-rich secretory protein-1 (CRISP-1; DE/AEG) and the novel related CRISP-3 are expressed under androgen control in the mouse salivary gland, *Endocrinology 133*, 192−198.
16. Udby, L., Calafat, J., Sørensen, O. E., Borregaard, N., and Kjeldsen, L. (2002) Identification of human cysteine-rich secretory protein 3 (CRISP-3) as a matrix protein in a subset of peroxidase-negative granules of neutrophils and in the granules of eosinophils, *J. Leukocyte Biol. 72*, 462−469.
17. Udby, L., Cowland, J. B., Johnsen, A. H., Sørensen, O. E., Borregaard, N., and Kjeldsen, L. (2002) An ELISA for SGP28/CRISP-3, a cysteine-rich secretory protein in human neutrophils, plasma, and exocrine secretions, *J. Immunol. Methods 263*, 43−55.
18. Ernst, T., Hergenhahn, M., Kenzelmann, M., Cohen, C. D., Bonrouhi, M., Weninger, A., Klaren, R., Grone, E. F., Wiesel, M., Gudemann, C., Kuster, J., Schott, W., Staehler, G., Kretzler, M., Hollstein, M., and Grone, H. J. (2002) Decrease and gain of gene expression are equally discriminatory markers for prostate carcinoma: a gene expression analysis on total and microdissected prostate tissue, *Am. J. Pathol. 160*, 2169−2180.
19. Tapinos, N. I., Polihronis, M., Thyphronitis, G., and Moutsopoulos, H. M. (2002) Characterization of the cysteine-rich secretory protein 3 gene as an early-transcribed gene with a putative role in the pathophysiology of Sjogren's syndrome, *Arthritis Rheum. 46*, 215−222.
20. Friess, H., Ding, J., Kleeff, J., Liao, Q., Berberat, P. O., Hammer, J., and Buchler, M. W. (2001) Identification of disease-specific

genes in chronic pancreatitis using DNA array technology, *Ann. Surg. 234*, 769−778.
21. Sørensen, O., Bratt, T., Johnsen, A. H., Madsen, M. T., and Borregaard, N. (1999) The human antibacterial cathelicidin, hCAP-18, is bound to lipoproteins in plasma, *J. Biol. Chem. 274*, 22445−22451.
22. Ishioka, N., Takahashi, N., and Putnam, F. W. (1986) Amino acid sequence of human plasma alpha 1B-glycoprotein: homology to the immunoglobulin supergene family, *Proc. Natl. Acad. Sci. U.S.A. 83*, 2363−2367.
23. Catanese, J. J., and Kress, L. F. (1992) Isolation from opossum serum of a metalloproteinase inhibitor homologous to human alpha 1B-glycoprotein, *Biochemistry 31*, 410−418.
24. Neves-Ferreira, A. G., Perales, J., Fox, J. W., Shannon, J. D., Makino, D. L., Garratt, R. C., and Domont, G. B. (2002) Structural and functional analyses of DM43, a snake venom metalloproteinase inhibitor from Didelphis marsupialis serum, *J. Biol. Chem. 277*, 13129−13137.
25. Rocha, S. L., Lomonte, B., Neves-Ferreira, A. G., Trugilho, M. R., Junqueira-de-Azevedo, I. de L., Ho, P. L., Domont, G. B., Gutierrez, J. M., and Perales, J. (2002) Functional analysis of DM64, an antimyotoxic protein with immunoglobulin-like structure from Didelphis marsupialis serum, *Eur. J. Biochem. 269*, 6052−6062.
26. Jurgilas, P. B., Neves-Ferreira, A. G., Domont, G. B., and Perales, J. (2003) PO41, a snake venom metalloproteinase inhibitor isolated from Philander opossum serum, *Toxicon 42*, 621−628.
27. Laemmli, U. K. (1970) Cleavage of structural proteins during the assembly of the head of bacteriophage T4, *Nature 227*, 680−685.
28. Towbin, H., Staehelin, T., and Gordon, J. (1979) Electrophoretic transfer of proteins from polyacrylamide gels to nitrocellulose sheets: procedure and some applications, *Proc. Natl. Acad. Sci. U.S.A. 76*, 4350−4354.
29. Lyngholm, J. M., Nielsen, H. V., Holm, M., Schiotz, P. O., and Johnsen, A. H. (2001) Calreticulin is an interleukin-3-sensitive calcium-binding protein in human basophil leukocytes, *Allergy 56*, 21−28.
30. O'Shannessy, D. J., Brigham-Burke, M., Soneson, K. K., Hensley, P., and Brooks, I. (1993) Determination of rate and equilibrium binding constants for macromolecular interactions using surface plasmon resonance: use of nonlinear least-squares analysis methods, *Anal. Biochem. 212*, 457−468.
31. Gill, S. C., and von Hippel, P. H. (1989) Calculation of protein extinction coefficients from amino acid sequence data, *Anal. Biochem. 182*, 319−326.
32. Lollike, K., Kjeldsen, L., Sengeløv, H., and Borregaard, N. (1995) Lysozyme in human neutrophils and plasma. A parameter of myelopoietic activity, *Leukemia 9*, 159−164.
33. Borregaard, N., Kjeldsen, L., Rygaard, K., Bastholm, L., Nielsen, M. H., Sengeløv, H., Bjerrum, O. W., and Johnsen, A. H. (1992) Stimulus-dependent secretion of plasma proteins from human neutrophils, *J. Clin. Invest. 90*, 86−96.
34. Gallagher, S. R. (1995) Native discontinuous electrophoresis and generation of molecular weight standard curves (Ferguson plots), in *Current Protocols in Protein Science* (Coligan, J. E., Dunn, B. M., Ploegh, H. L., Speicher, D. W., and Wingfeld, P. T., Eds.) Unit 10.3.5−10.3.11, John Wiley & Sons, New York.
35. Neves-Ferreira, A. G., Cardinale, N., Rocha, S. L., Perales, J., and Domont, G. B. (2000) Isolation and characterization of DM40 and DM43, two snake venom metalloproteinase inhibitors from Didelphis marsupialis serum, *Biochim. Biophys. Acta 1474*, 309−320.
36. Schultze, H. E., Heide, K., and Haupt, H. (1963) Isolation of an easily precipitable alpha1-glycoprotein of human serum, *Nature 200*, 1103.
37. Eiberg, H., Bisgaard, M. L., and Mohr, J. (1989) Linkage between alpha 1B-glycoprotein (A1BG) and Lutheran (LU) red blood group system: assignment to chromosome 19: new genetic variants of A1BG, *Clin. Genet. 36*, 415−418.
38. Gahne, B., Juneja, R. K., and Stratil, A. (1987) Genetic polymorphism of human plasma alpha 1B-glycoprotein: phenotyping by immunoblotting or by a simple method of 2-D electrophoresis, *Hum. Genet. 76*, 111−115.
39. Halaby, D. M., and Mornon, J. P. (1998) The immunoglobulin superfamily: an insight on its tissular, species, and functional diversity, *J. Mol. Evol. 46*, 389−400.
40. Stratil, A., Kalab, P., and Pokorny, R. (1988) Evidence for the presence of alpha 1B-glycoprotein in mammalian sera: immunoblotting studies, *Comp. Biochem. Physiol. 91*, 783−788.

BI048823E